Geology, Geophysics & Environment 2022, vol. 48 (2): 111–132

Attribute analysis as a tool for determining the areas of the late diagenetic Main Dolomite deposits and assessing the stability of the seismic signal parameters

Norbert Smalera

AGH University of Science and Technology, Faculty of Geology, Geophysics and Environmental Protection, Krakow, Poland; Polish Oil and Gas Company, Exploration and Production Branch, Piła, Poland; e-mail: norbert.smalera@gmail.com, ORCID ID: 0000-0002-4584-9089

Received: 7 February 2022; accepted: 22 May 2022; first published online: 2 June 2022

Abstract: The results of the lithofacial analysis of data from the Moracz 3D seismic survey were among the main premises leading to the positioning of the new petroleum exploration well in that area. Unfortunately, the reservoir properties of the drilled part of the Main Dolomite carbonates differed significantly from those anticipated by the analysis of the amplitudes of the seismic signal recorded. Such surprisingly negative results impelled the reinterpretation of 3D seismic data. Hence, a number of analyses of the amplitudes, the frequencies, and the variability of phase shift were carried out in order to determine the influence of these parameters on the lithofacial interpretation of seismic data. The results revealed a fundamental error of amplitude with the extraction maps. It appeared that the distribution of amplitudes is not essentially controlled by the reservoir properties of the Main Dolomite carbonates but by the fault shadow effect coming from Mesozoic graben in the overburden. In addition, a large diversity of frequency spectra was found, which, combined with the small thickness of the exploration level, could have contributed to incorrect identification of seismic reflections. There was also a change in seismic signatures from the same reflection in different parts of the survey, raising doubts about the distribution of the phase rotation. In order to recognize phase rotation diversity, a new seismic data analysis was based upon the selected Triassic sediments of high impedance. The obtained maps demonstrated significant variability within the data volume due to attenuation. The reinterpreted data from the Moracz 3D seismic survey proved the uneven and unstable distribution of amplitudes, frequencies, and phase which resulted in erroneous conclusions of petroleum exploration. After modeling with the use of different frequency ranges, an analysis of the amplitude extraction of the horizons related to the Main Dolomite was performed. Then the amplitude ratio attribute was selected which eliminated the influence of the regional amplitude and frequency distribution and showed the distribution of dolomite properties more reliably than the amplitude extraction maps.

Keywords: seismic attributes, Zechstein, Main Dolomite, fault shadow, dominant frequency, phase shift map, attenuation

INTRODUCTION

Seismic attributes are all the information obtained from seismic data, either by direct measurements or by logical or experience-based reasoning (Taner 2001). The evolution of seismic attributes is closely linked to advances in computer technology (Chopra & Marfurt 2005). Dynamic progress has been made since the 1970s, when computers were first applied to geophysical

data processing and interpretation. There are now 300 kinds of computable seismic attributes, and the number of commonly used attributes is 50–60 (Li & Zhao 2014). According to Brown (2011), the principal information provided by seismic attributes includes time, amplitude, frequency, and attenuation. In Poland, seismic attributes have also become the principal recognition tool of rock formations in the subsurface. Górski & Trela (1997) analysed BMB, the biggest Polish oil field, using seismic attributes. Dec & Pietsch (2012) described the key factors in their paper for the identification of gas accumulations in carbonates in Fore Sudetic Monocline. Kwolek & Mikołajewski (2010) highlighted the fact that, besides geometrical criteria, the analyses of seismic reflections are crucial in the identification of the litofacial traps. Zdanowski & Górniak (2014) focused on dim spots and bright spots as indicators of hydrocarbon reservoirs. All of these papers have a common geological target, namely the Main Dolomite (Ca2).

Seismic attribute methodology was also used in the Polish Shoreland region (Fig. 1) where the Moracz 3D seismic survey project was conducted in 2014 (Zych 2014). This survey covered the area of the Wysoka Kamieńska oil field as well as the Stawno petroleum prospect (Fig. 2). Later, in 2017, the Stawno-1 well on the Stawno structure was completed west of the Wysoka Kamieńska oil field. The promising features of the Stawno prospect were confirmed by the presence of a structural trap and by the results of seismic attribute analysis. The latter indicated the presence of the Zechstein Main Dolomite facies of favorable reservoir properties (Zych 2014). Such dolomites encountered in the adjacent Wysoka Kamieńska oil deposit revealed porosity sometimes exceeding 20% and saturation with oil. Moreover, in that oil play, late diagenetic dolomites (Ca2_pd) were distinctly discernible from the underlying, non-porous and impermeable grey limestones. The close vicinity of oil deposits proved the full development of a petroleum system and suggested the possibility of hydrocarbon accumulations. Unfortunately, drilling through the Main Dolomite, which was the crucial hydrocarbon exploration target, did not confirm the presence of the

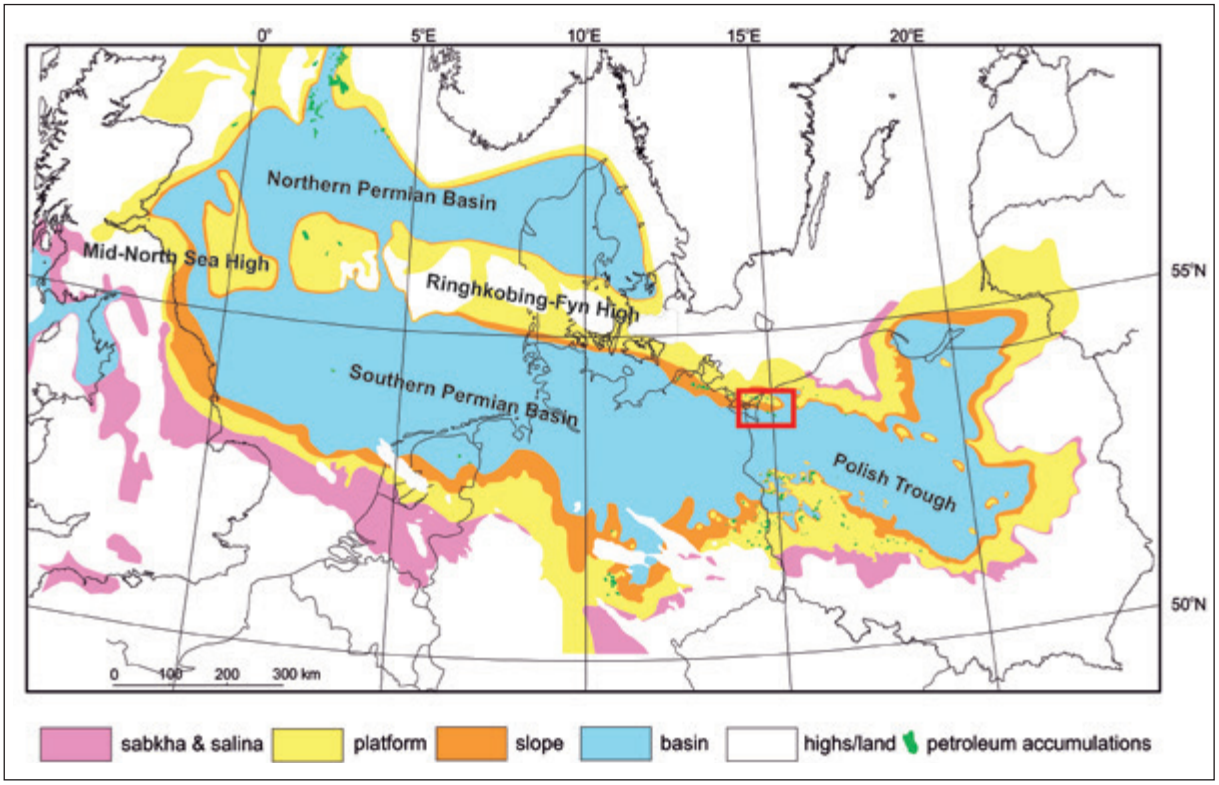

Fig. 1. *Paleoenvironmental map of the Zechstein Carbonate in the Southern Permian Basin, NW Europe, in Late Permian time (Słowakiewicz et al. 2015 modified). Red rectangle marks the study area*

perspective late diagenetic dolomites with high porosities. Shortly after drilling the Stawno-1 well, the question arose as to why the seismic attributes provided such promising values in that specific region, indicating the improved reservoir properties of carbonates within the explored Stawno structure, and on its southern slope. The aim of this paper is to answer this question. The analysis of the source data shows that the Mesozoic graben had a large impact (a fault shadow effect) on the amplitudes and frequencies. Additionally, the phase rotation in this area is controlled by attenuation. These factors resulted in erroneous conclusions from the seismic attribute analysis. The modeling carried out shows that it is possible to calculate seismic attribute analysis in conditions that better reflect the distribution of properties in the studied area than the standard amplitude extraction methodology for the Main Dolomite.

Geological setting

The study area is located in the NW part of Polish Trough (Fig. 1). Three main structural stages were distinguished in that region: Variscan, Permian-Mesozoic, and Cenozoic. In the area of the Moracz 3D seismic survey, the oldest rocks were Carboniferous sediments only encountered in the Moracz-IG1 well. These strata were covered by Autunian lavas and pyroclastics followed by Saxonian clastics.

The second structural stage included four Zechstein cyclothems: Werra, Stassfurt, Leine, and Aller (Wagner 1994), showing various thicknesses and lithologies: mostly rock salt, anhydrites as well as thin dolomite, limestone, and claystone layers (Fig. 3). The high contrasts of the impedance of Zechstein deposits creates a number of seismic reflections. The most important are Z2 (seismic top of Basal Anhydrite), Ca2str (seismic top of late diagenetic Main Dolomite), and Ca2sp (seismic base of late diagenetic Main Dolomite) (Fig. 3). The Main Dolomite, which is the most promising level in this area, is covered by the Basal Anhydrite (A2) unit, which shows insignificant thickness and high velocity contrast and, thus, it relatively efficiently reflects the structural pattern of the Main Dolomite.

Zechstein is covered with thick Mesozoic sediments represented by the Triassic, Jurassic and the Cretaceous. The Mesozoic formations lying on the Permian formations underwent quite significant disturbances.

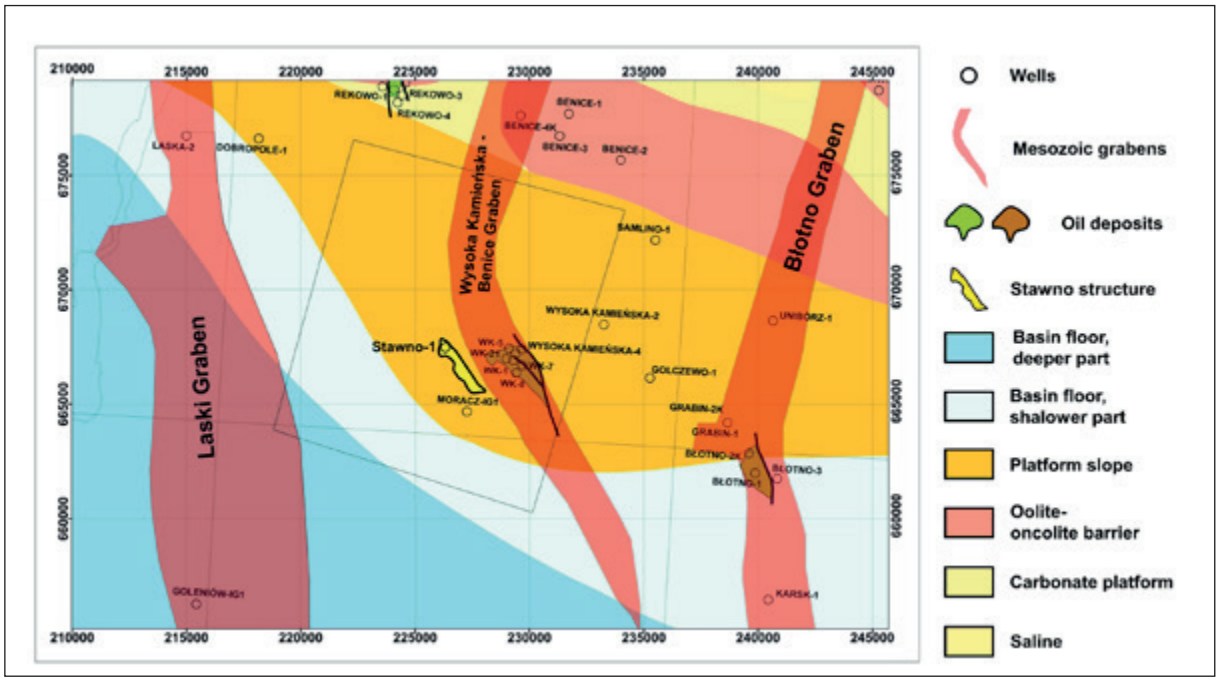

Fig. 2. *Location map of the study area (black rectangle) referred to the part of paleogeographic map of the Main Dolomite in Poland (Wagner et al. 2000 modified) and integrated with the sketch map of Mesozoic tectonic structures (Knieszner et al. 1998). Black line marks the seismic section displayed in Figure 4*

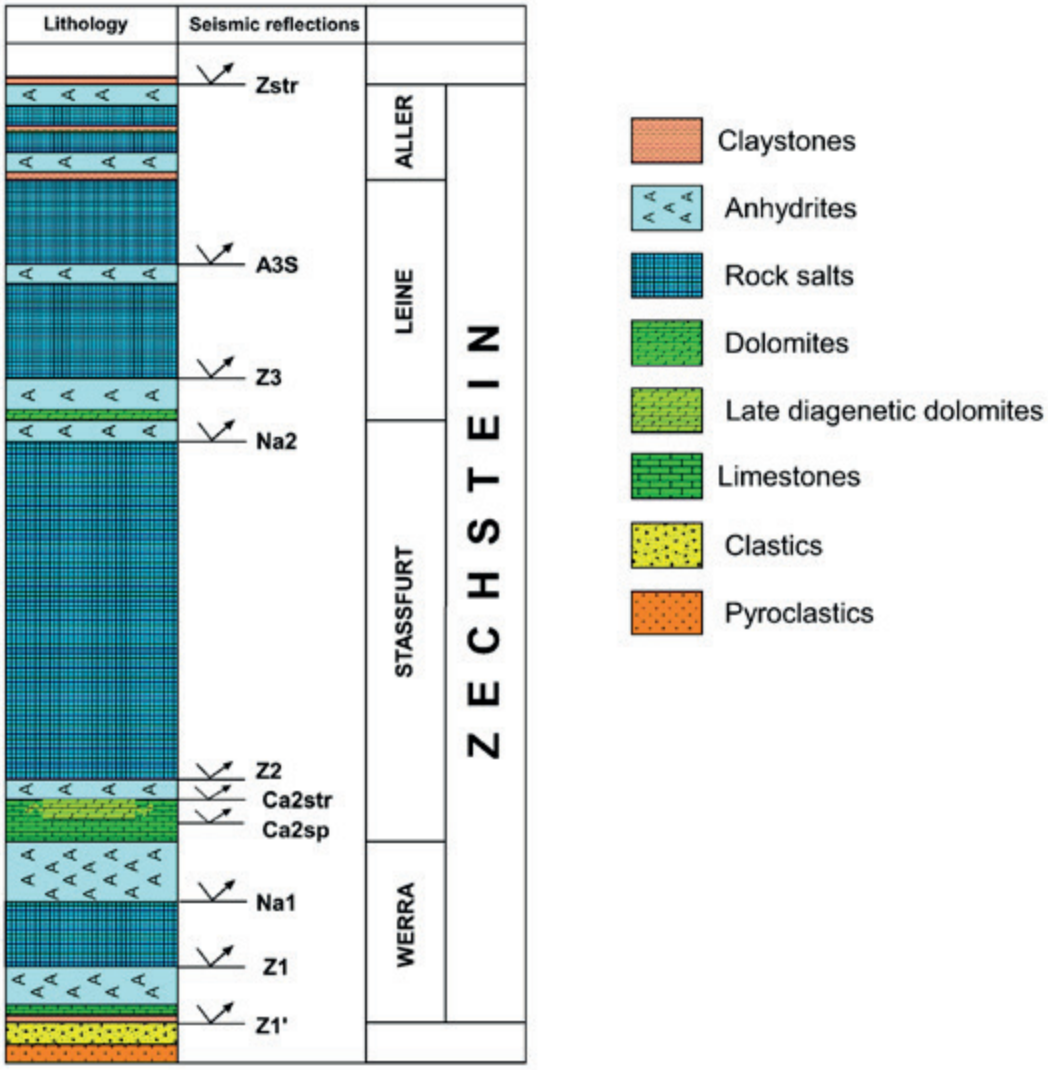

Fig. 3. *Zechstein cyclothems succession. Seismic reflections: Zstr – top of Zechstein, A3S – top of Middle Anhydrite, Z3 – top of Main Anhydrite, Na2 – top of Older Halite, Z2 – top of Basal Anhydrite, Ca2str – top of late diagenetic Main Dolomite, Ca2sp – base of late diagenetic Main Dolomite, Na1 – top of Oldest Halite, Z1– top of Lower Anhydrite, Z1' – base of Zechstein*

As a result of these movements and the denudation process, high deficiencies in the continuity of the sediments (Keuper, Rhaetian) and large differences in the thickness of individual links were found, especially in the area of the Mesozoic graben zone and its edges (Ślemp & Gamrot 2013) (Fig. 4). The most important Mesozoic tectonic structures in the study area are the Wysoka Kamieńska – Benice Graben (WKBG) (Figs. 2, 4) and the fault zone located in the southern part of the surveyed area (Fig. 4). In this area, the Triassic consists of Buntsandstein (Tp), Muschelkalk (Tm), Keuper (Tk), and Rhaetian (Tre). The Buntsandstein is represented by sandstones, claystones, mudstones, and anhydrite inserts. One of the key Triassic seismic boundaries used for the purposes of this work is the base of a thin layer of anhydrite and, at the same time, the top of the Middle Buntsandstein sandstones (Tp2). This reflection, however, does not appear in the WKBG. There is a Muschelkalk above the Buntsandstein which is built by high velocity limestones, dolomites and thin anhydrites. Keuper, and Rhaetian are made of claystone with gypsum and anhydrite inserts. The Jurassic is made up of sandstones, claystones, and mudstones with a small amount of carbonates. The Cretaceous mudstones, claystones, and sandstones deposits were found only in the profiles of the boreholes located on the SW from the Wysoka Kamieńska oil field.

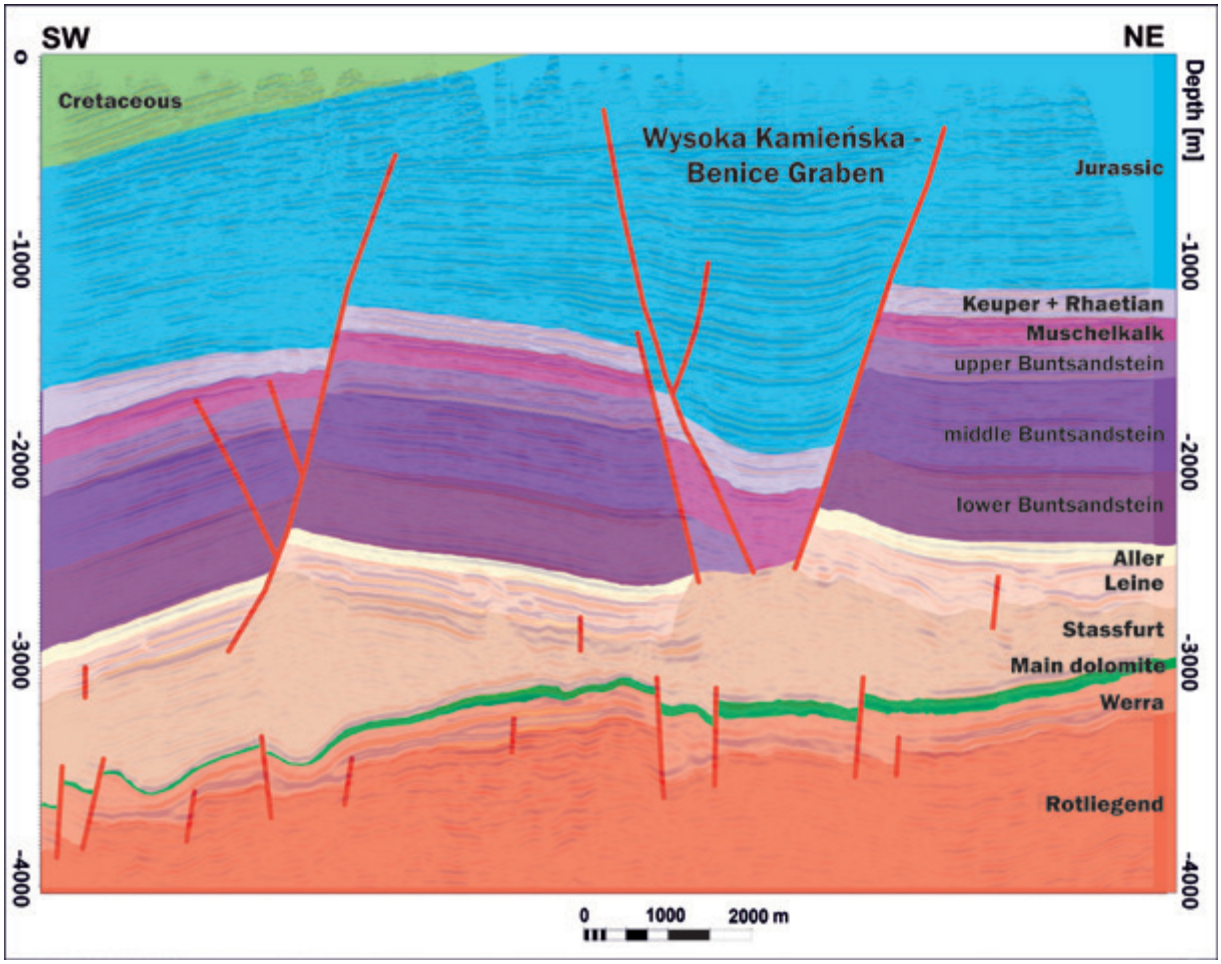

Fig. 4. *Arbitrary interpreted seismic section*

The erosive surface of the Mesozoic deposits is covered with small thicknesses of clays, sands, and gravels of the Kenozoic.

Petroleum geology

From the hydrocarbon exploration point of view, the most important is the Zechstein Stassfurt cyclothem, which embraces the Main Dolomite. In northwestern Poland, several oil deposits have been discovered in that lithostratigraphic unit, e.g.: Błotno, Gorzysław, Kamień Pomorski, Międzyzdroje, Petrykozy, Rekowo and Wapnica (Dyjaczyński et al. 2006; Mikołajewski 2008). In the eastern part of the Moracz 3D seismic survey area, the Main Dolomite carbonates accumulated the Wysoka Kamieńska oil deposit in the basin slope zone (Fig. 2). Analyses demonstrated that carbonates were good petroleum source rocks due to the increased content the of organic matter (Mikołajewski et al. 2012). Additionally, the hydrocarbon migration pathways were very short (Kotarba & Wagner 2007). Because the reservoir rocks showed very low porosity and low permeability, the Wysoka Kamieńska oil field was included into the fractured category (Karnkowski 1993). However, the results of detail research proved that the Wysoka Kamieńska oil deposit is reservoired within the zone of late diagenetic dolomites, of porosity which sometimes exceeds even 20% (Mikołajewski & Gamrot 2014). Moreover, the properties of the reservoir rocks were closely controlled by the presence of Mesozoic grabens in the overburden (Kniesznerr et al. 1998). Tectonic movements might have facilitated the invasion of aggressive surface waters into the rock formations. As the Main Dolomite carbonates were sealed by the rock salt and anhydrite formations, the circulating waters might have decisively modified their reservoir properties (Kniesznerr et al. 1998).

Methods

The interpreted datasets comprised the results of 3D seismic survey and the well data. In the study area, the Moracz 3D seismic survey project was completed in 2014. That survey integrated the results of new field data acquisition with those from the Wysoka Kamieńska 3D seismic project completed in 2001 (central east part, close to Wysoka Kamieńska wells). The Wysoka Kamieńska 3D seismic survey was acquired with a brick pattern. The distance between the shot lines was 600/200 m and receiver lines 400 m. The shot and receiver array spacing was 50 m. For the active patch, the offset inline was 3000 m and the corresponding crossline was 2200 m. The seismic wave field was sampled in the bin of size 25 m × 25 m. The fold for this survey was 26 ±2. The Moracz 3D seismic survey was also acquired with a brick pattern. The distance between the shot lines was 450 m and receiver lines 300 m. The shot and receiver array spacing was 50 m. For the active patch, the offset inline was 3125.5 m and the corresponding crossline was 2975.3 m. The seismic wave field was sampled in the bin of size 25 m × 25 m. The fold for this survey was 70. The datasets subjected to interpretation were pre stack time migration (1) AGC (automatic gain control) volumes with the rescaled amplitudes and (2) RAP volumes with the preserved relative relationships of amplitudes. Data from nine wells within the Moracz 3D project area also were taken into account. Eight of them were done in the years 1978–1985. The well logs from this period are of poor quality. Only three wells (Stawno-1, Moracz-IG1, and Wysoka Kamieńska-8) drilled the Main Dolomite in its entirety, but only Wysoka Kamieńska-8 drilled the late diagenetic dolomites. In only these three wells were measurements of the Dt in Main Dolomite, the results of which were used for modelings. RHOB measurements were conducted only in the Stawno-1 well, which were used to determine the density in the modelings. The other wells provided data on A2, Ca2, and Ca2_pd thickness. The first part of the analyzes was focused on examining seismic data in terms of the amplitude, frequency, and phase rotation distribution. In order to investigate these three factors, the following were created: (1) RMS volume, (2) a map of the dominant frequency, and (3) a map showing the spatial distribution of phase rotation. The second part of the analyzes focused on the spatial recognition of areas with improved Ca2 properties. Several modelings of seismic traces were carried out. The modelings aimed to recognize which features of seismic records would be sensitive to the increasing thickness of late diagenetic dolomites within the Main Dolomite unit. Finally, based on the modelings, the extraction maps and the amplitude ratio map were computed and submitted to detailed analysis.

RESULTS

Source data analysis

As mentioned above, two seismic data volumes, AGC and RAP, were available. Although the RAP data processing methodology used was aimed at preserving the true relationships between the amplitudes, these methods failed. RMS amplitude distribution for the RAP volume demonstrated the presence of vertical zones of decreased and increased amplitudes (Fig. 5). The computed attribute was the root of the mean amplitude squared for the RAP seismic volume, for 33 ms gate. A decrease of amplitudes was related to the presence of Mesozoic WKBG and a fault, with both destructively affecting the distribution of amplitudes (Fig. 5).

During the extraction of a seismic signal for calculations of synthetic seismograms, variable spectrum of frequencies was found within the seismic volume. Figure 6 shows the map of extraction for the Z2 seismic boundary from the volume of instantaneous dominant frequency calculated for 33 ms time gate. This attribute is defined as the square root of the sum of the squares of instantaneous frequency and instantaneous bandwidth (Barnes 1993). It shows the mean frequency that can be obtained for a given sample when the frequency spectrum is calculated for a given gate. In the northeastern and western parts of the study area, and in the vicinity of the Moracz-IG1 well, much higher dominant frequencies occur in comparison with the southern part of the area or the zone of the WKBG.

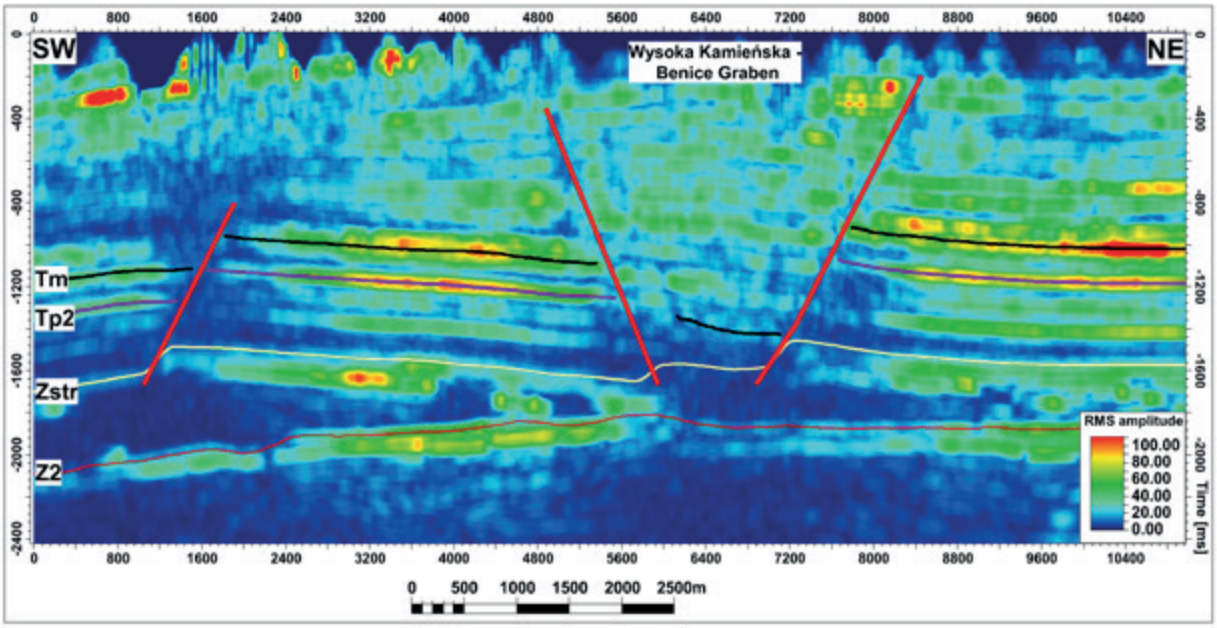

Fig. 5. *Arbitrary seismic section (RMS attribute version) calculated from the RAP volume for 33 ms gate: Tm – top of Muschelkalk, Tp2 – top of Middle Buntsandstein, Zstr – top of Zechstein, Z2 – seismic top of Basal Anhydrite*

Figure 7 demonstrates the influence of a variable frequency spectrum on seismic data. In areas where lower dominant frequencies were recorded, the seismic reflections are wider and the resolution is lower. This causes the problem of separating the upper Na1 side lob, from the potential bottom Ca2_pd. In the vicinity of the Moracz-IG1 well (high dominant frequencies marked in Figure 7 on S side), where higher frequencies were preserved, it was possible to discriminate between the side lobe from the top surface of the Oldest Halite (Na1) unit and the positive reflection located above, the latter representing the potential bottom seismic boundary of porous dolomites Ca2_pd. In the southern part (zone C in Figure 6) low dominant frequencies were found. In this area the Ca2sp and upper Na1 side lobe were not separated despite the thickness similar to that in the vicinity of Moracz-IG1.

Taking into account the fact that a variable distribution of amplitudes and variable frequency spectra were observed in the Moracz 3D seismic survey it was possible that a variable phase distribution occurred as well. During the data analysis, signatures of seismic reflections were checked in the vicinity of Triassic seismic boundaries, from which the Tp2 (i.e., the bottom of a thin layer of high impedance within the Triassic Buntsandstein formation) was the subject for more detailed considerations. In the northwestern part of that surveyed area, in the vicinity of the Tp2 reflection interpreted as a negative amplitude, the minus-plus signature was observed (Fig. 8). However, in the southeastern part of the surveyed area, on both sides of the fault, this signature changed into minus-plus-minus in the vicinity of the Rokita structure. The seismic record highlighted the quiet depositional conditions. Moreover, the compaction of the rock formation was insufficient to change the distribution of seismic velocities within the sediment layers as various patterns of seismic reflections were evident at similar depths. Hence, the only explanation consistent with both the results of analysis of Triassic seismic boundaries and the uncertain seismic records from the Zechstein formation was the variable phase of the seismic signal.

The analysis of the attributes was carried out with the assumption that both the thickness distribution and the development of sediments outside the WKBG area are similar. First, the Tp2 seismic boundary was interpreted before the ratio of amplitudes of peaks adjacent to that reflection was calculated.

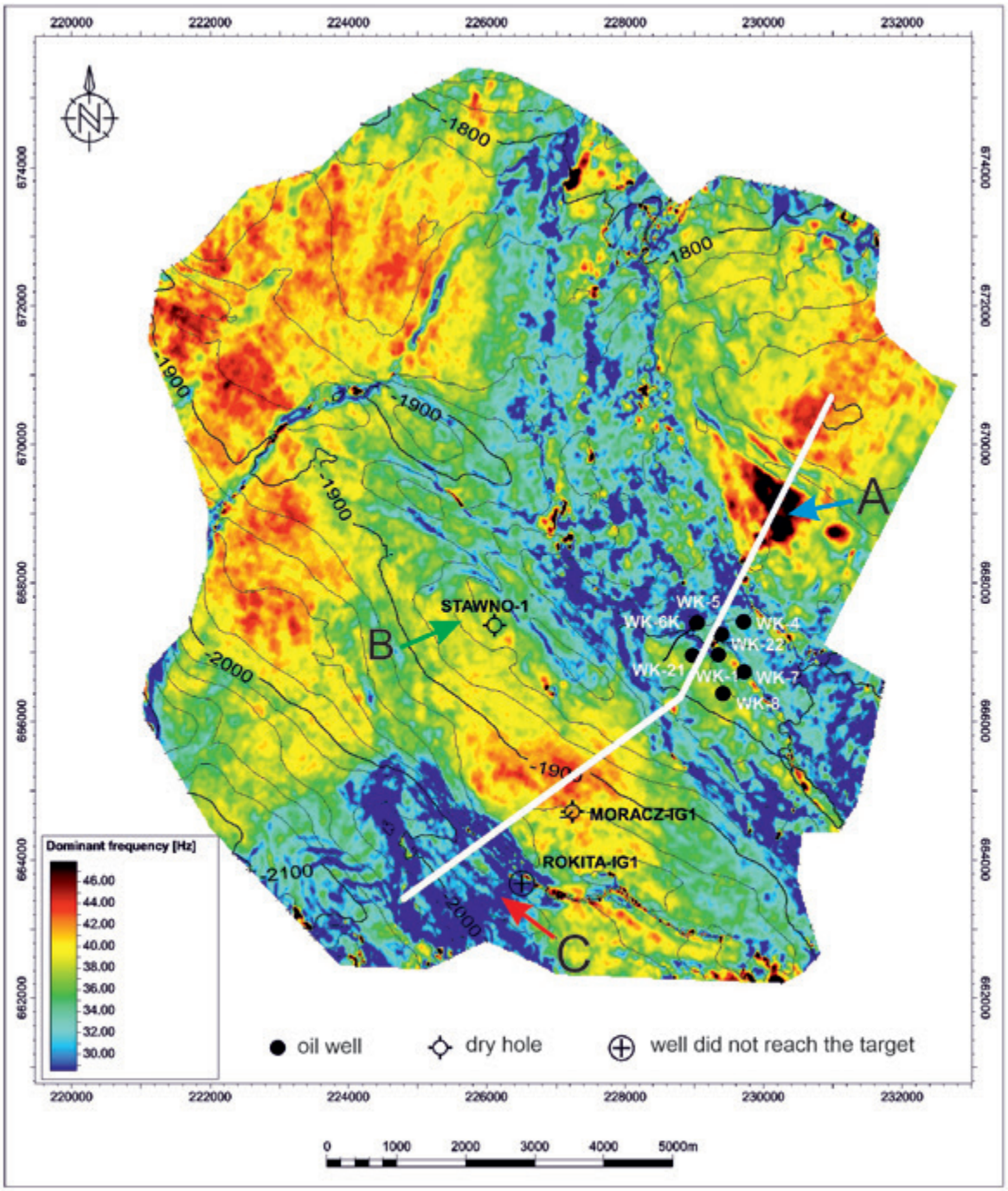

Fig. 6. *Map of amplitude extraction for the Z2 seismic boundary from dominant frequency volume calculated from the AGC volume for 33 ms gate. White line marks position of seismic line in Figure 7. Isochrones of Z2 seismic boundary. A,B,C marks the areas from which signals have been extracted for the modeling in Figure 10*

The WKBG could not be included in this analysis due to the changes in thicknesses of particular lithostratigraphic units. In part of the graben, the Tp2 reflection is most likely not present at all. In the remaining part it most likely interfered with other reflections from the Triassic, which disqualifies it from this type of analysis. The results of calculations are illustrated in Figure 9, which documents the changing ratios of first peak amplitude above Tp2 (Tp2t) divided by first peak amplitude below Tp2 (Tp2b) over the area of the seismic survey. This ratio also indirectly illustrates the phase shift within the data volume.

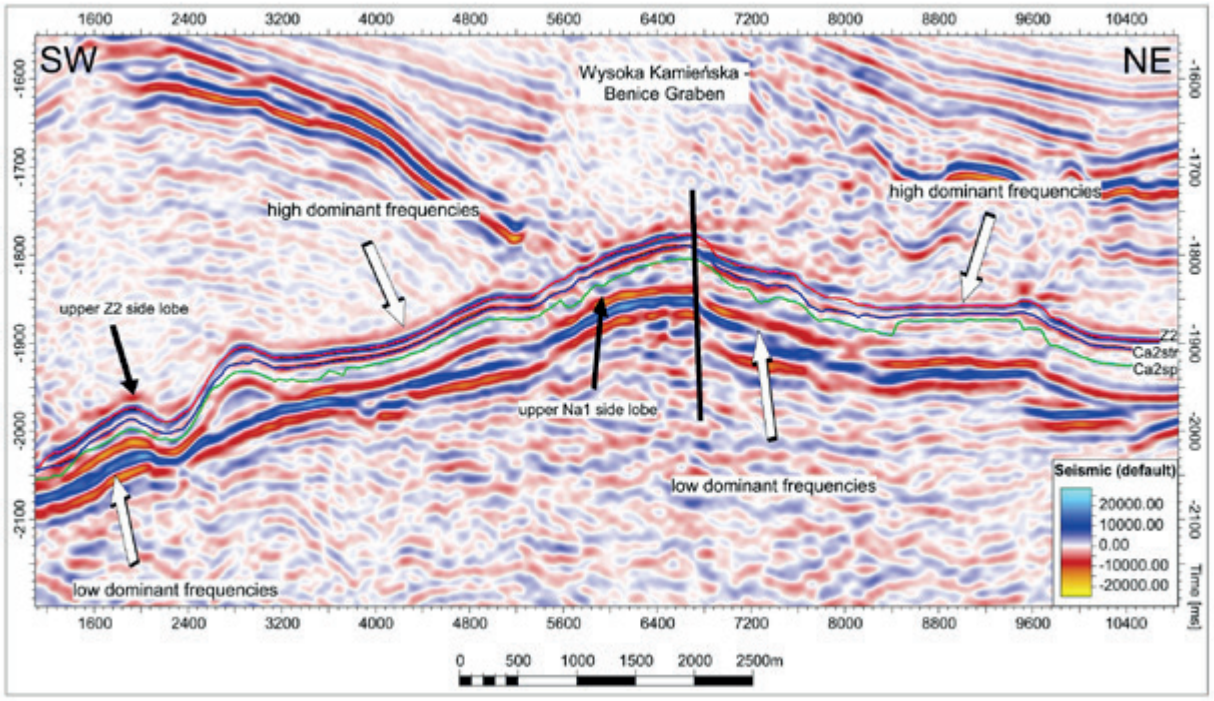

Fig. 7. *Arbitrary seismic line derived from the AGC volume: Z2 – seismic top of Basal Anhydrite, Ca2str – potentially seismic top of late diagenetic Main Dolomite, Ca2sp – potentially seismic base of late diagenetic Main Dolomite, Na1 – seismic top of Oldest Halite*

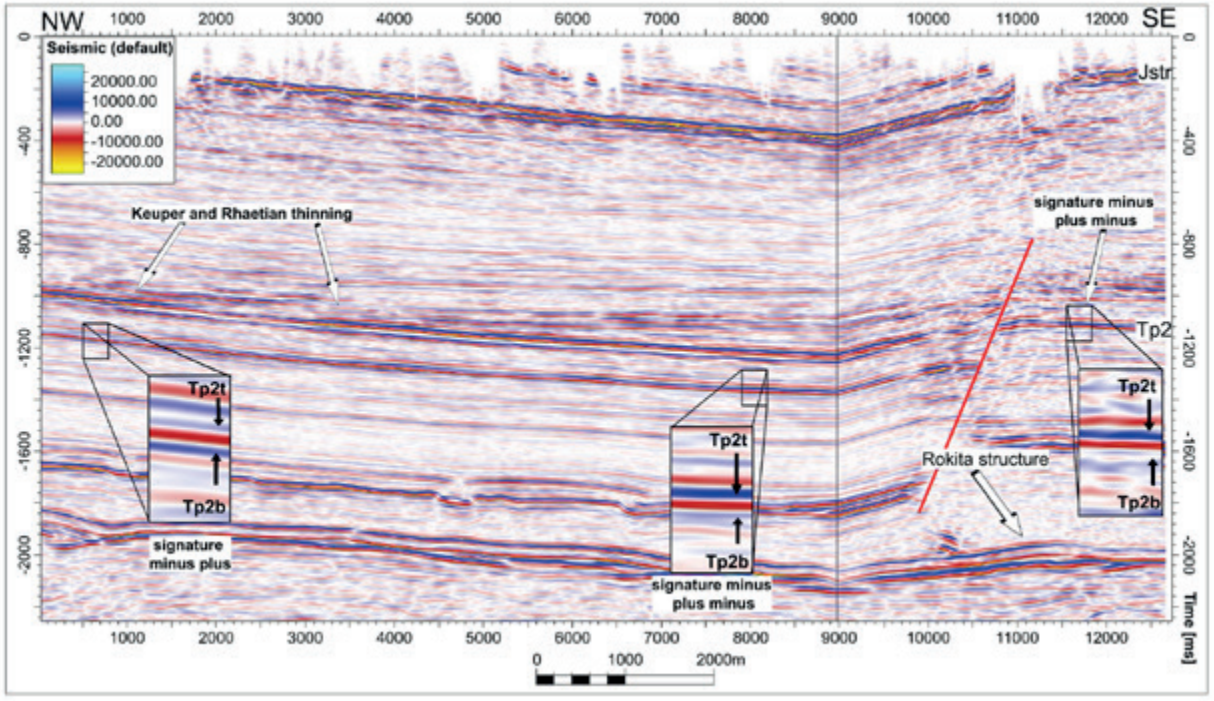

Fig. 8. *Arbitrary seismic section illustrating the phase variability within the 3D data volume: Jstr – top of Jurassic, Tp2 – top of Middle Buntsandstein, Tp2t – peak amplitude above Tp2, Tp2b – peak amplitude below Tp2. Red line – interpreted fault*

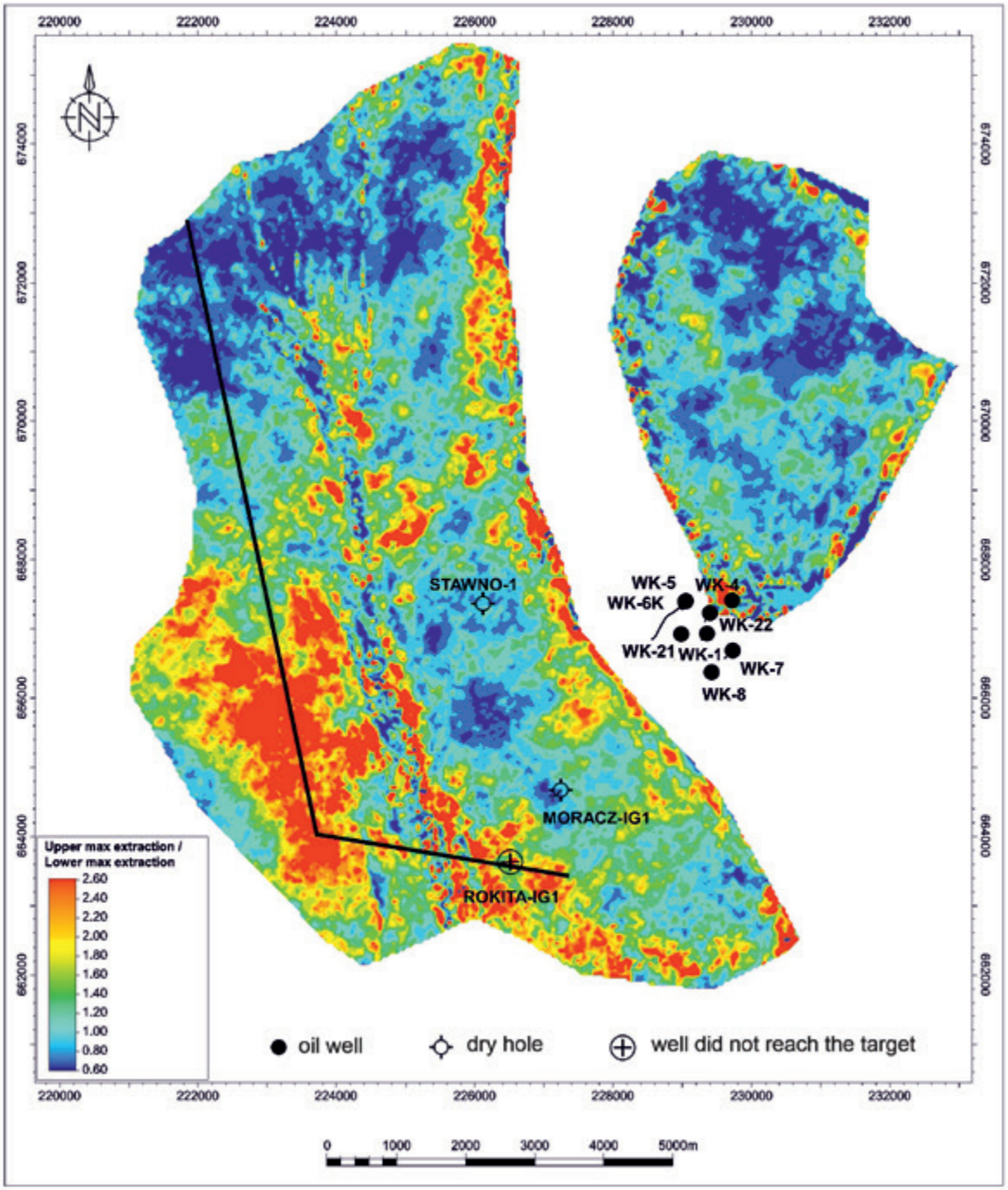

Fig. 9. *Map of the ratio of amplitude extraction of the closest maxima above and beneath the Tp2 seismic reflection. Black line marks the seismic section shown in Figure 8*

The results show that the Stawno-1 and the Moracz-IG1 wells are located in the same zone, which means that phase shift parameters calculated from both wells are not representative for the entire study area (Fig. 9). At this stage of the study, variable phase shift cannot be applied for the given data volume, and the areas of different values of phase shift must be interpreted individually.

Modeling

Despite the irregular amplitude, frequency, and phase distribution found during the analysis of the source data, an attempt was made to determine

the distribution of reservoir properties in the area of the Moracz 3D survey. The starting point for the analysis was the construction of the model of rock formation that was based on the mean thicknesses from the nine wells in the area. The model comprised seven layers corresponding to the following Zechstein stratigraphic units (from the bottom): Lower Anhydrite (A1d) (42 m), Oldest Halite (Na1) (40 m), Upper Anhydrite (A1g) (85 m), bipartite Main Dolomite (Ca2), comprising late diagenetic dolomites (Ca2_pd) (0–15 m) and carbonates with poor reservoir properties (Ca2_b) (65 m), Basal Anhydrite (A2) (8 m), and Older Halite (Na2). The geological model was filled with the velocities and densities from the Dt logs (converted to P wave velocity) from the Stawno-1, Moracz-IG1, and Wysoka Kamieńska-8 wells (Fig. 3) and RHOB log from Stawno-1 well. The densities and velocities for anhydrites were 2.95 g/cm^3 and 6000 m/s, for halites 2.07 g/cm^3 and 4500 m/s, for Ca2_pd 2.3 g/cm^3 and 4400 m/s, and for Ca2_b 2.7 g/cm^3 and 6100 m/s. The signal was extracted from three areas with different frequency characteristics, which had different values on the map of dominant frequency (A, B, C in Figure 6). The signals were extracted using a statistical method from the Zechstein interval, before their spectrums were modeled using a trapezoidal spectrum. With this methodology, insignificant changes between the extracted and model signals were noted. The signal from area A was represented by the frequency spectrum 13–33–46–85 Hz, from area B 5–30–35–80 Hz, and from C 5–22–23–65 Hz. The geological model combined with the well logs (density and P-wave velocity) and the seismic signal led to the calculation of synthetic seismograms using the convolution function. Several data analyses were carried out and selected results are displayed in Figure 10, which illustrates the seismic trace modelings for variable thickness of the Ca2_pd member and frequency spectrums. The conducted tests enabled us to determine three main seismic features, which reflect the improvement of reservoir properties or the increasing thickness of late diagenetic dolomites:

– decrease of positive amplitude of Z2 reflection from the top surface of the Basal Anhydrite (A2) (i.e., from the interface with the Older Halite Na2);
– increase of negative amplitude in the top of the Ca2_pd member;
– increase of positive amplitude in the base of the Ca2_pd member.

The above conclusions are in line with the results of analyzes carried out by Górski & Trela (1997), Kwolek & Mikołajewski (2010), Dec & Pietsch (2012), and Zdanowski & Górniak (2014) in other regions concerning the Main Dolomite.

One additional observation was made when analyzing the model of the thinning layer at different frequency spectra. It was found that the amplitude ratio of upper side lobe of Z2 (uZ2) (red arrows in Figure 10) to the Z2 amplitude itself (violet arrows in Figure 10) increases with increasing Ca2_pd thickness. The Z2 side lobe to Z2 is less sensitive to frequency changes than Ca2sp and Ca2str reflections, especially at small Ca2_pd thicknesses. Even the insignificant thickness of Ca2_pd member resulted in decrease of amplitude of the Z2 reflection whereas the side lobe remained unchanged for each of the frequency spectra.

Considering the results of the modeling reported above, identification of the areas where the Ca2 dolomites have more favorable reservoir properties required the application of amplitude attributes. The extraction of amplitude values from seismic RAP volume for the following seismic horizons: Z2 (Fig. 11), Ca2str (Fig. 12), and Ca2sp (Fig. 13) was carried out. Selected horizons are displayed in Figure 7.

Two of the three applied attributes indicated the improved reservoir properties and the increased thickness of dolomites in the vicinity of the Stawno-1 well and SE of it (a black circle in Figures 11–13). It is observed by high negative amplitudes of Ca2str, and high positive amplitudes of Ca2sp. The modelings shows that the greater the amplitudes at the top and bottom of Ca2_pd, the greater the thickness of the late diagenetic dolomite (Fig. 10). In the eastern part of the seismic survey area, where the Wysoka Kamieńska oil deposit is located and Ca2_pd is present, the amplitudes extracted for Ca2str and Ca2sp horizons were relatively low (red circle in Figures 12, 13). Thus, the increased thickness of the Ca2_pd member and/or the improvement of reservoir properties of dolomites could be expected in the vicinity of the Stawno-1, as the amplitudes are higher.

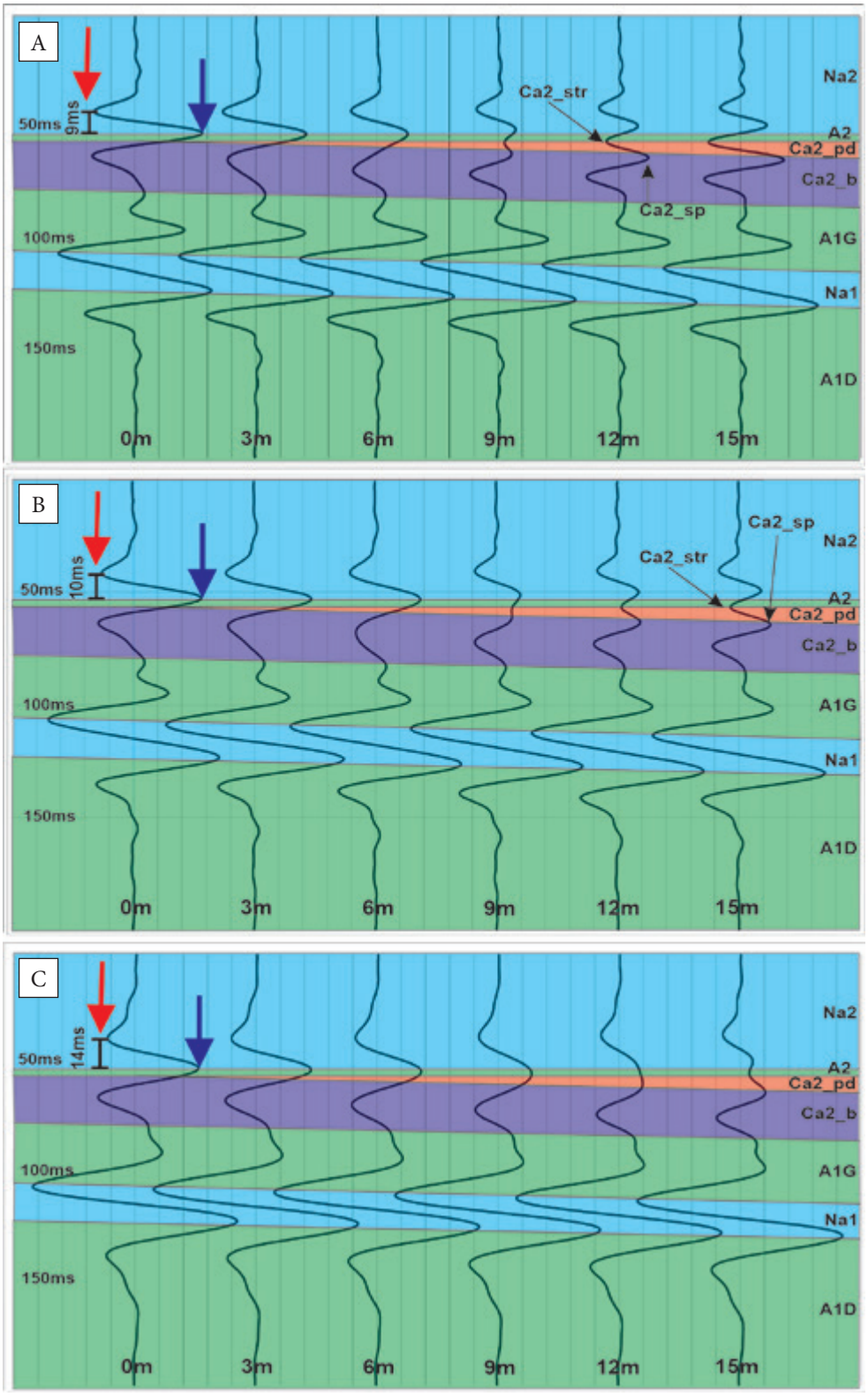

Fig. 10. *Synthetic seismograms calculated for the model considering the changes of thickness of late diagenetic dolomites. Signal with a trapezoidal frequency spectrum: A) 13–33–46–85 Hz; B) 5–30–35–80 Hz; C) 5–22–23–65 Hz. The A, B, C letters correspond to the areas marked in Figure 6. Violet arrows mark Z2 central peak, red arrow mark side lobe of Z2 reflection. Na2 – Older Halite, A2 – Basal Anhydrite, Ca2_pd – late diagenetic dolomite, Ca2_b – carbonates of poor reservoir properties, A1G – Upper Anhydrite, Na1 – Oldest Halite, A1D – Lower Anhydrite, Ca2str – seismic top of late diagenetic dolomite, Ca2sp – seismic base of late diagenetic dolomite*

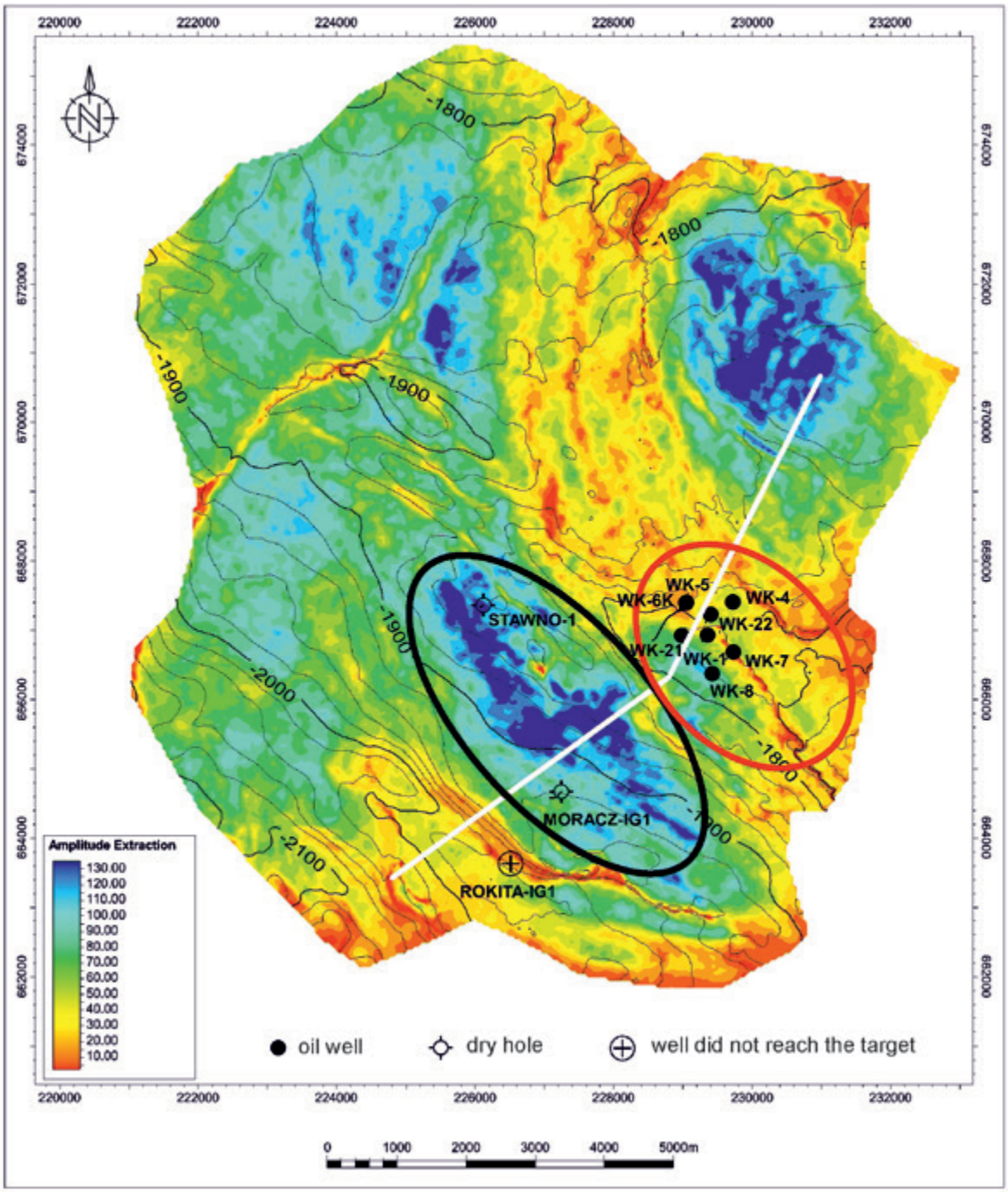

Fig. 11. *Map of extracted amplitude values from RAP volume for the Z2 seismic boundary. Black ellipse marks the anomaly related to the Stawno structure, red ellipse marks the Wysoka Kamieńska oil deposit area, white line marks an arbitrary seismic line displayed in Figure 7. Isochrones of Z2 seismic boundary*

However, the amplitudes extracted for the Z2 seismic boundary revealed increased values, which indicates the absence of late diagenetic dolomites from the modelings.

Taking into consideration the regional amplitude distribution noted during the analysis of the source data, it was decided to check whether the amplitude distributions Z2, Ca2str and Ca2sp duplicate the regional amplitude distribution or whether they are independent. In order to verify it, the amplitude was extracted for the Zstr boundary (Fig. 8). In most of the analyzed seismic survey area, this was the claystone/rock salt interface.

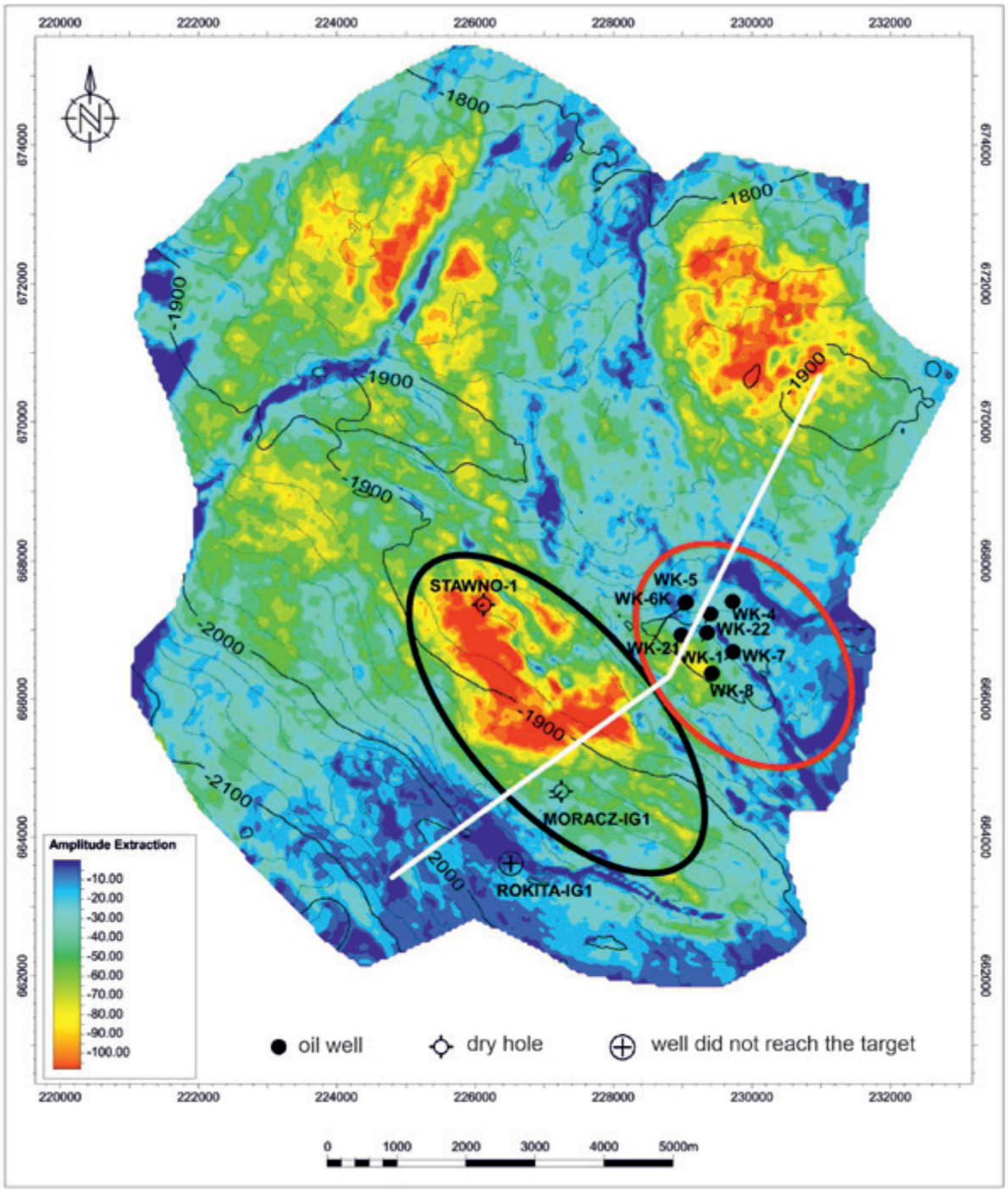

Fig. 12. *Map of extracted amplitude values from RAP volume for the Ca2str seismic boundary. Black ellipse marks the anomaly related to the Stawno structure, red ellipse marks the Wysoka Kamieńska oil deposit area, white line marks an arbitrary seismic line displayed in Figure 7. Isochrones of Ca2str seismic boundary*

The obtained pattern was similar to that observed on the maps of extracted amplitudes for Z2, Ca2str and Ca2sp boundaries. This result confirmed that the regional distribution of amplitudes is controlled by the presence of Mesozoic graben and not by the distribution of reservoir properties within the Main Dolomite Ca2 unit. Therefore, the separate interpretation of the maps of extracted amplitudes for Z2, Ca2str, and Ca2sp seismic boundaries is groundless and may lead to erroneous exploration conclusions.

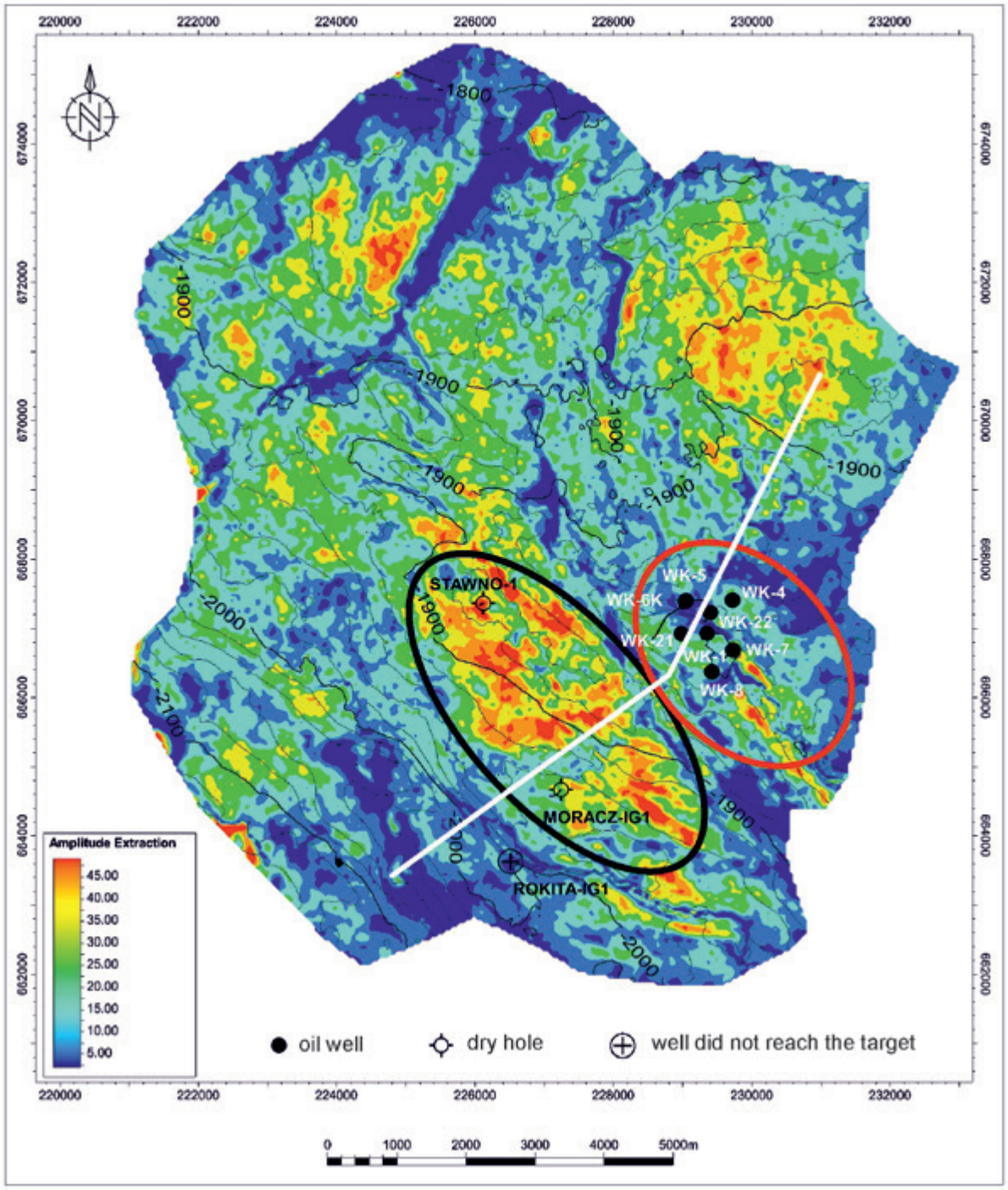

Fig. 13. *Map of extracted amplitude values from RAP volume for the Ca2sp seismic boundary. Black ellipse marks the anomaly related to the Stawno structure, red ellipse marks the Wysoka Kamieńska oil deposit area, white line marks an arbitrary seismic line displayed in Figure 7. Isochrones of Ca2sp seismic boundary*

The last observation that was made during the modeling was that the amplitude ratio from uZ2 to Z2 can be a method of determining the Ca2_pd occurrence zones. Disturbances in the amplitude distribution of the seismic volume noted on RMS section (Fig. 5) and confirmed by the similarity of the extraction amplitude maps Z2 (Fig. 11), Ca2str (Fig. 12), and Ca2sp (Fig. 13) to the Zstr (Fig. 14), have a regional distribution both horizontally and vertically. The amplitude quotient of adjacent reflections eliminates the regional trend.

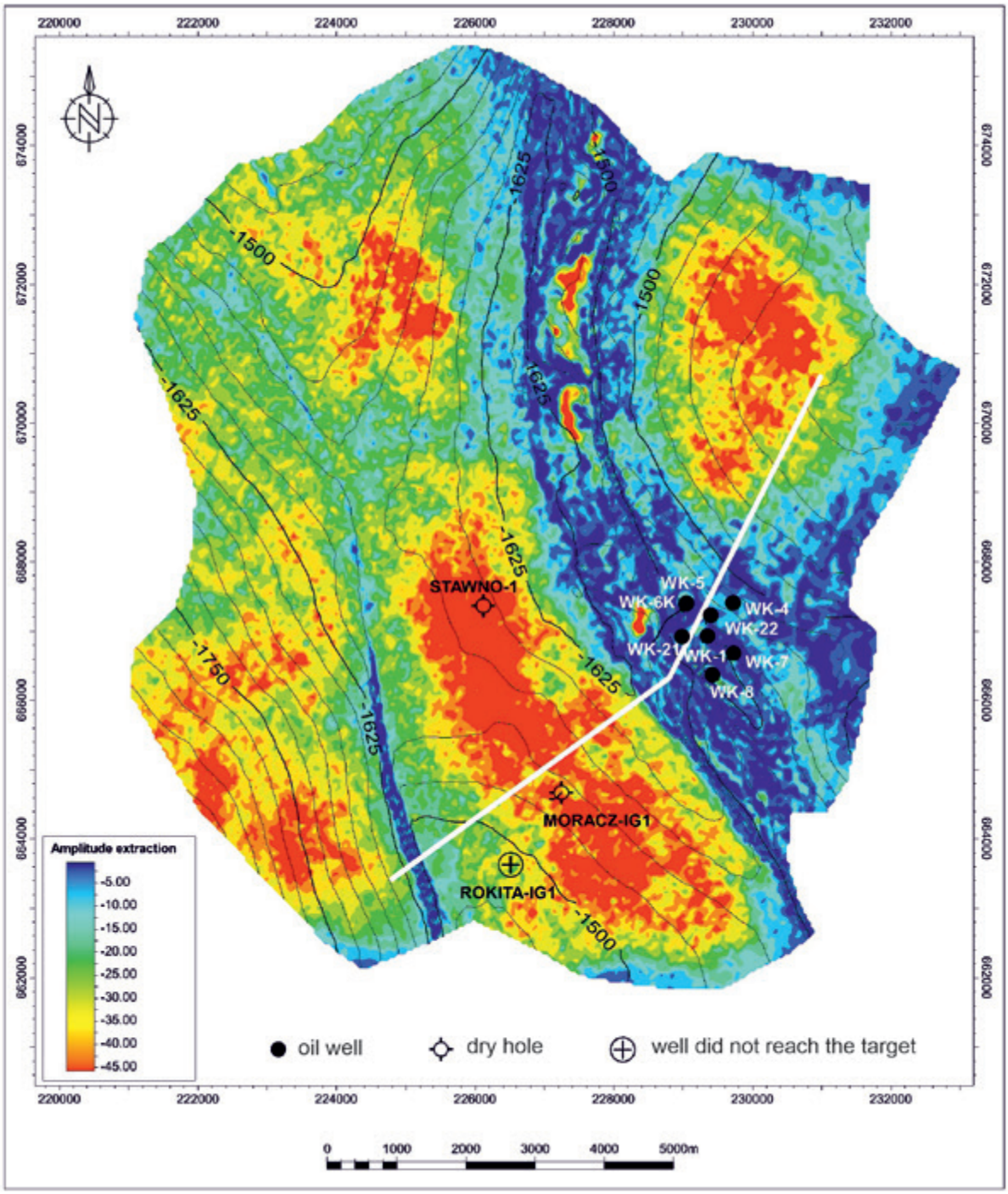

Fig. 14. *Map of amplitude extracted from RAP volume for the Zstr seismic boundary. White line marks the seismic line displayed in Figure 7. Isochrones of Zstr seismic boundary*

The modelings revealed that the best prospective areas should be located at the sites of its high negative values, where the amplitude of Z2 reflection is close to that of the side lobe. On the map (Fig. 15), such an area was identified southeast of the cluster of wells around the Wysoka Kamieńska oil field and in the southern part of the surveyed area, in the vicinity of the Rokita-IG1 well. Unfortunately, that well did not penetrate the Ca2 unit due to technical failures, which precluded the recognition of the petrophysical properties of the Main Dolomite.

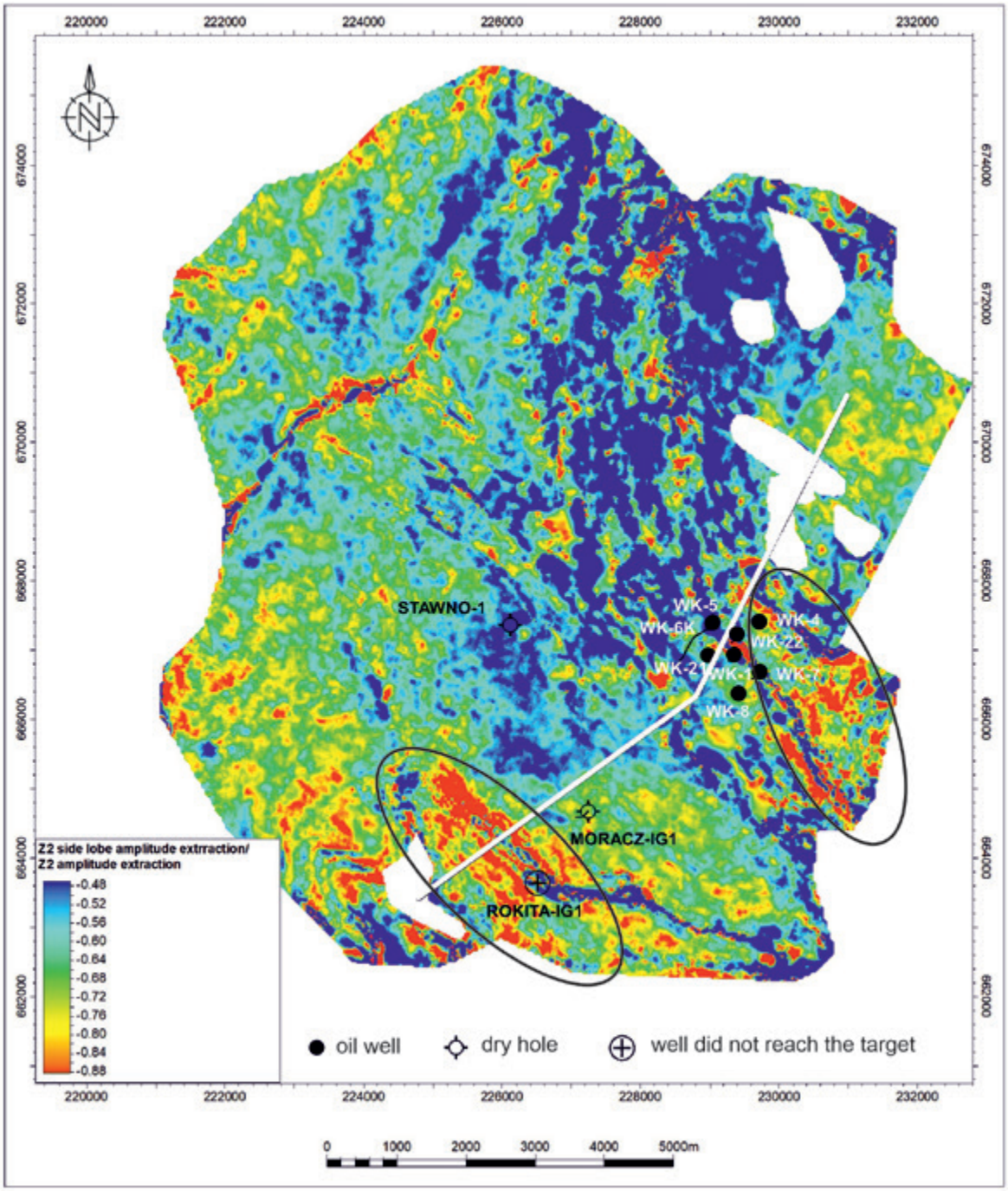

Fig. 15. *Map of the ratio of amplitudes extractions of the Z2 upper lobe and the Z2 reflection. White line marks the seismic line displayed in Figure 7. Black ellipse marks the anomaly in vicinity to the Rokita, violet ellipse marks the anomaly near Wysoka Kamieńska oil deposit area*

DISCUSSION

The amplitude decreases observed in the seismic volume are mainly related to WKBG and the fault in SW. The zone of unreliable seismic imaging in the footwalls is what is known as the fault shadow zone. It can occur in all types of faults, but the term is usually applied to extensional faults (Fagin 1996). Seismic rays traveling through fault areas experience geometrical and travel time distortions which result in poor seismic images and non-hyperbolic moveout anomalies in areas below such fault planes

(Birdus 2007). The major part of this problem is caused by rapid lateral velocity changes within fault zones (Julien et al. 2000). In the case of Moracz 3D seismic survey, Muschelkalk (Tm) is the high velocity layer that generates the fault shadow effect. As can be seen in Figure 5, especially in the central part and in the NE, amplitudes above the Tm reflection have a uniform distribution and the disturbances begin just below it. In the SW part, there is most likely an overlapping of two effects, the fault shadow and the amplitude attenuation from Cretaceous or Jurassic, and therefore the amplitudes in this part are additionally lowered above Tm. Seismic disturbance zones may have several distinct explanations: (1) inappropriate illumination during the acquisition, (2) the incorporation of diffractive components during the stacking procedure, and (3) an inappropriately simplified velocity model within the deformed area (Iacopini et al. 2016). As research on this problem shows, the best solution is to use depth migration before stacking with a detailed velocity model (Birdus & Artyomov 2010, Michel et al. 2011, Nie et al. 2012). In the Moracz 3D survey, a pre stack time migration was applied that did not cope with the fault shadow effect. In order to eliminate this effect or reduce its impact, the recommendation is to reprocess data using depth migration before stacking.

The dominant frequency distribution (Fig. 6), similarly to the amplitude distribution in the region of WKBG and the fault in SW, is controlled mainly by the fault shadow phenomenon described above. The relatively elevated values of the dominant frequency observed in the vicinity of Wysoka Kamieńska as compared to the rest of the WKBG may be related to the frequency tuning. The instantaneous frequency becomes anomalously high when bed thickness is about a quarter period and remains high as the bed continues to thin (Robertson & Nogami 1984). The increase in the instantaneous frequency will cause the increase of the dominant frequency, which may indicate that the thickness of the late diagenetic dolomite in this zone reaches 1/4 of the wavelength or less. On the other hand, many studies (Tai et al. 2009, Li & Rao 2020, Renhai et al. 2021) indicate that attenuation of high frequencies (frequency shadow) may occur below gas and oil reservoirs together with a lowering of the dominant frequency. Due to the occurrence of the Mesozoic graben in the overburden and fault shadow effect, it is difficult to assess whether frequency tuning or frequency shadow effects occur and on what scale.

The map of the amplitude extraction ratio from above and below Tp2 reflection (Fig. 9) indirectly demonstrate the phase rotation distribution in the seismic image. It shows a zone of increased values around 2.5 (Fig. 9 – red colour values), which crosses the fault in the SW part of the survey. Local disturbances can be seen at the fault, but the regional trend continues through it, as is the case in the WKBG zone. Therefore, the regional distribution of phase rotation is not controlled by the fault shadow phenomenon, and most likely attenuation is the main factor that influences its spatial distribution. The attenuation of the wave is directly linked to the different layers that compose the Earth, so that whenever changes in the composition of layers occur, the attenuation also changes (Hedlin & Margrave 2004). The attenuation is progressive in the sense that the propagating wavelet continuously experiences high frequency attenuation and associated phase shifts as it propagates (Margrave 2016). In Figure 8, the thinning of Keuper and Rhaetian is indicated, which may be the cause of a change in attenuation. The second level which may be responsible for the unstable attenuation may be the Cretaceous which occurs above the Jstr (top of Jurassic) boundary (Fig. 8) and also has an uneven thickness distribution in the study area. It is very difficult to determine which of these levels is responsible for the variable distribution of the phase rotation. It would be possible to determine it if there was an amplitude stable boundary between the Jstr boundary and Tp2, on the basis of which similar analyses could be performed as in the case of the Tp2. If the results were consistent with the results obtained from the Tp2 analyses, it would mean that the cause of the variable phase rotation would be the Cretaceous layer. Unfortunately, no such boundary could be found. The elimination of the variable phase rotation distribution is possible with the use of advanced processing procedures taking into account Q compensation (Bano 1996, Wang 2008) and reprocessing with the use of these procedures is a recommendation for the Moracz 3D survey.

According to the Rayleigh criterion, the seismic resolution is the time difference between the central peak (marked with violet arrow for Z2 reflection in Figure 10) and the closest negative side

lobe (marked with red arrow for Z2 reflection in Figure 10) (Kallweit & Wood 1982). In the study area, this time difference varies between 9–14 ms in Zechstein. If the seismic velocity in the porous dolomite Ca2_pd was assumed as about 4400 m/s (for the Basal Anhydrite A2 unit it was 6000 m/s), its corresponding seismic thickness varied from 19.8 m to 30.8 m (for the A2 unit it was 27–42 m). Regretfully, such values far exceeded both the measured and the anticipated thicknesses of the A2 (<15 m) unit and the Ca2_pd member (<9 m). From the modeling (Fig. 10) it appears that Ca2str is identified as the first negative reflection below Z2, this is true for a Ca2_pd thickness of around 12 m for the signal from zone A (Fig. 6) and over 15 m (about 20 m) for the signal from zone C (Fig. 6). In the case of low thicknesses of Ca2_pd and the small amount of high frequencies, Ca2str could be misidentified with the side lobe of A2. The increasing negative value of Ca2str would be the sign of increased thickness of Ca2_pd or its improved reservoir properties (Fig. 10) but only for Ca2_pd thicknesses above 12–20 m. Identification of the true bottom surface of the late diagenetic dolomites is also problematic. The modelings (Fig. 10) showed that, reflection from the bottom surface of late diagenetic dolomites should be the first positive reflection beneath the Z2 seismic boundary. The modelings (Fig. 10) also showed that the determination of the Ca2sp was possible if Ca2_pd thickness was at least 12 m for a signal extracted from zone A (Fig. 6) and for zone C this thickness would exceed 15 m (about 20 m). For lower Ca2_pd thicknesses, it appeared very possible that the interpreted Ca2sp would in fact represent the side lobe of the Oldest Halite unit or the second lobe from Z2. However, if such a distinction is possible, the increased positive amplitudes of this reflection may indicate the improvement of reservoir thickness of the Ca2_pd. If the thickness of the entire dolomite were low and Ca2_pd was present, it is possible that the upper side lobe of Na1 and Ca2sp would be merged.

In the Moracz 3D survey, where there are small Ca2_pd thicknesses (<9 m), reflections from its top and bottom are difficult to distinguish from side lobes and noises, especially with a variable frequency range (Fig. 10). Even if in some part of the 3D survey these reflections are related to the presence of Ca2_pd with larger thicknesses, it is difficult to distinguish where this occurs. This thesis is confirmed by the result of the Stawno-1 well where no Ca2_pd has been drilled and Ca2str and Ca2sp where interpreted (Figs. 12, 13). In this case, the maps of the amplitude distribution of Ca2str and Ca2sp do not represent the distribution of the Ca2 dolomite properties and should not be taken into account in the analysis of this issue. The only indicator of the presence of the Ca2_pd is the reduction of the amplitude of the Z2 reflection. The modeling (Fig. 10) shows that, regardless of the frequency spectrum, an increase in Ca2_pd thickness is associated with a decrease in the Z2 amplitude. The interpretation revealed that low amplitude value of the Zechstein Z2 reflection was an effect of the strong interference of reflections from the top surfaces of the A2 unit and the Ca2_pd member. However, such a lowering was only observed at insignificant thickness of the Basal Anhydrite A2 unit, below the tuning value (i.e., below the thickness at which the maximum amplification of amplitudes occurs for adjacent reflections of opposite polarities). If the A2 unit was thick (i.e., above the tuning value) the reflections would be independent and the Z2 amplitude would only represent the properties of anhydrite, and the overlying rock salt unit.

The solution to fault shadow problem seemed to be the application of attributes calculated as ratios of amplitudes extracted for close seismic boundaries. In this case it was the ratio of the amplitudes of the uZ2 to Z2. As shown in Figure 5, the attenuation of amplitudes, both vertical and horizontal, was a regional feature in the study area. As the Z2 and its upper side lobe remained within short time distance from each other, the disturbance of seismic signal caused by fault zones located in the overburden similarly affected both. Therefore, the quotient of extracted amplitudes eliminated the regional trend and enhanced the features of seismic records related to the presence of late diagenetic dolomites Ca2_pd. AGC (256 ms gate) applied to one of the analyzed volumes increased the amplitudes on a regional scale and, like the regional weakening caused by the fault shadow, could be eliminated by the amplitude ratio. It does not matter whether the amplitude ratio is extracted from the AGC or RAP volume, both give the same results because the amplitude ratios are the same on a local scale. However, the ratio

of the amplitudes of the uZ2 to Z2 will be ineffective at the sites where thickness of Older Halite Na2 unit is low and where the multiple reflections interfere with the side lobe or Z2. In both cases, the interference will disturb the relationships of amplitudes. The basic presumptions of the effectiveness of that method are: (1) the occurrence of porous/fractured dolomite in the top part of the Main Dolomite unit, (2) low thickness of the Basal Anhydrite unit, and (3) stable phase within the analyzed seismic volume. If these conditions are not met, the attribute will be ineffective.

According to the map of the ratio of amplitude extractions of the uZ2 and the Z2 reflection (Fig. 15), the vicinity of the Rokita-IG1 well appeared to be the most prospective target for petroleum exploration. Several tests were carried out in order to match the seismic records and the generated synthetic seismograms in the vicinity of the Rokita-IG1 well. The essential problem was the sufficient fit of the results of modelings of rock formations to the seismic records acquired for the Z2–Z1' stratigraphic interval (i.e., the bottom of the Zechstein). The adjustment of seismic velocities in the Upper Anhydrite A1g unit was challenging because velocity estimated from the modelings was about 5300 m/s whereas its measured value in the vicinity was about 6000 m/s. An attempt was made to interpret this gap as the effect of pressure from the underlying Oldest Halite Na1 succession, which triggered the infilling of generated fractures with the rock salt. This might have lowered the seismic velocity in the A1g unit. However, the analysis of similar structures and well logs revealed that velocities in the A1g unit remained constant. An alternative explanation could be the lowering of seismic velocity caused by the increased thickness of dolomites of favorable reservoir properties but the analysis of regional geological setting made this concept rather improbable. According to the regional geological map (Wagner et al. 2000), a transition is evident in the shallow part of sedimentary basin in the vicinity of the Rokita-IG1 well, accompanied by the deterioration of the reservoir properties of dolomites. In the overburden of the Main Dolomite Ca2, a fault is present (Fig. 8), along which the migration of fluids might have occurred causing the formation of late diagenetic dolomites. However, if this concept is true the thickness of dolomites must have been about 80 m whereas their thickness measured in the Wysoka Kamieńska oil deposit is only several meters. Apparently, other factors must play a role in this process. The map of amplitude extraction of the closest maxima above and beneath the Tp2 seismic reflection (Fig. 9), the vicinity of the Rokita-IG1 well revealed high values, in contrast to other parts of the study area. This map indirectly shows up something about phase rotation. Thus, the phase shift by 50° was applied, which enabled the fit the modeled and the rotated seismic traces observed near the well. This methodology led to the calculation of impedance parameters of the Main Dolomite Ca2 unit with a high degree of probability. The obtained values demonstrated the absence of the desired porous dolomites interval or its very insignificant thickness. The second zone, in which the improved reservoir properties of the Main Dolomite were implied, was identified in the vicinity of the Wysoka Kamieńska well cluster (Fig. 11). Unfortunately, the presence of tectonic graben in the overburden precluded the determination of the phase shift in this area. In addition, data with reduced quality from the older Wysoka Kamieńska survey was used at the processing stage in this zone. Certainly, the very close vicinity of the Wysoka Kamieńska deposit is an advantage, however, it is difficult to assess the prospectiveness of this zone on the basis of seismic attributes.

CONCLUSIONS

The analyzes of seismic data showed that there is an uneven distribution of amplitudes, frequencies and phase shift in the Moracz 3D survey area which was the reason for erroneously drawn conclusions from the analyzes carried out before drilling the Stawno-1 well. If even one of these factors is omitted during the attribute analysis, the conclusions from the search regarding both the desired Ca2_pd thickness and the favorable reservoir properties will be incorrect. The regional pattern of amplitudes and frequencies is mainly controlled by the fault shadow phenomenon caused by the high velocity Muschelkalk layer. This phenomenon manifests itself in a reduction of the amplitudes on the RAP volume and the attenuation of high frequencies (drop in resolution) in footwall blocks in WKBG and in the fault in the S part of the survey. Additionally, a variable distribution of phase rotation was found in the research

area, resulting from the attenuation phenomenon. At this stage of the analysis, it is impossible to discriminate whether the attenuation causing the phase rotation is due to the Keuper and Rhaetian deposits or the Cretaceous. The modelings showed that in the case of small thicknesses of Ca2_pd, reflections from its top and bottom may be confused with side lobes from the Basal Anhydrite and the Oldest Halite reflections, especially in zones with a limited range of high frequencies. Due to the regional distribution of amplitudes unrelated to the Ca2_pd deposits and the possibility of erroneous identification of its top and bottom, individual maps of amplitude extraction from the Z2, Ca2str, and Ca2sp horizons cannot determine perspective zones. The best determinant of zones with the possible occurrence of late diagenetic Ca2 deposits is the ratio of the amplitude from the uZ2 to the Z2. The calculation of the amplitude ratio of adjacent reflections eliminates the regional distribution of amplitudes. In addition, it does not matter whether the RAP or AGC volume is used for calculations because ratio changes are based on local amplitude distribution. The modeling shows that the amplitude ratio of uZ2/Z2 is good for low Ca2_pd thicknesses and is independent of the frequency spectrum in the Moracz 3D seismic volume. The uneven distribution of phase rotation detected during the analysis of seismic data have a negative impact on the interpretation of the uZ2/Z2 ratio. Variable phase shift cannot be applied at this stage and the areas of different values of phase shift must be interpreted individually. An example is the Rokita structure where the values of the uZ2/Z2 were increased, but it resulted from a different phase rotation than originally adopted. Unfortunately, apart from the zone to the east of the Wysoka Kamieńska wells, where it was not possible to conduct phase rotation analyzes, it was not possible to select any zones with good Ca2 properties. It is possible that such zones are only present in the area of the Wysoka Kamieńska oil deposit or that the thickness of the Ca2_pd member is so insignificant that it cannot be discerned by seismic records. Moreover, it cannot be precluded that dolomites with a different structure are present in the study area, and thus that zones with favorable reservoir properties simply do not occur in the topmost part of the Ca2 succession. If so, a series of comprehensive modelings is recommended which would help in determining the attributes relevant to the identification of the position of late diagenetic dolomites. Additional modeling of the A2 thickness and the location of the Ca2_pd layer in the entire Ca2 profile should be performed. A recommendation for possible future work in this area is also to perform data reprocessing with the use of depth migration, which would eliminate or reduce the fault shadow effect, and attenuation compensation which could eliminate the uneven distribution of the phase rotation.

REFERENCES

Barnes A.E., 1993. Instantaneous spectral bandwidth and dominant frequency with applications to seismic reflection data. *Geophysics*, 58, 3, 419–428. https://doi.org/10.1190/1.1443425.

Bano M., 1996. Q-phase compensation of seismic records in the frequency domain. *Bulletin of the Seismological Society of America*, 86, 4, 1179–1186. https://doi.org/10.1785/BSSA0860041179.

Birdus S., 2007. Removing fault shadow distortions by fault-constrained tomography. *SEG Technical Program Expanded Abstracts*, 26, 3039–3043. https://doi.org/10.1190/1.2793102.

Birdus S. & Artyomov A., 2010. Fault shadow distortions on 3D seismic data and their removal by depth processing. *ASEG Extended Abstracts*, 1, 1–4. https://doi.org/10.1081/22020586.2010.12041843.

Brown A., 2011. *Interpretation of Three-Dimensional Seismic Data*. 7th ed. AAPG Memoir, SEG Investigation in Geophysics, 9, Society of Exploration Geophysicists and the American Association of Petroleum Geologists. https://doi.org/10.1190/1.9781560802884.

Chopra S. & Marfurt K.J., 2005. Seismic attributes – A historical perspective. *Geophysics*, 70, 5, 3–28. https://doi.org/10.1190/1.2098670.

Dec J. & Pietsch K., 2012. Możliwości sejsmicznej identyfikacji stref akumulacji gazu w utworach węglanowych cechsztynu monokliny przedsudeckiej. *Gospodarka Surowcami Mineralnymi – Mineral Resources Management*, 28, 93–112. https://doi.org/10.2478/v10269-012-0025-z.

Dyjaczyński K., Mamczur S. & Dziadkiewicz M., 2006. *Od Rybaków do L-M-G: 45 lat wydobycia ropy naftowej na Niżu Polskim*. [w:] *Materiały Konferencji „50 lat poszukiwań ropy naftowej i gazu ziemnego w północno-zachodniej Polsce: tradycja i nowe wyzwania: konferencja naukowo-techniczna, Piła 1–2 VI 2006"*, Bogucki Wydawnictwo Naukowe, Poznań, 59–76.

Fagin S., 1996. The fault shadow problem: Its nature and elimination. *The Leading Edge*, 15, 9, 1005–1006. https://doi.org/10.1190/1.1437403.

Górski M. & Trela M., 1997. Układ geometryczny i ocena właściwości serii zbiornikowej złoża Barnówko-Mostno-Buszewo (BMB) – największego złoża ropy naftowej w Polsce – na podstawie zdjęcia sejsmicznego 3D. *Przegląd Geologiczny*, 45, 7.

Hedlin K.J. & Margrave G., 2004. Seismic Attenuation Problem. [in:] Bohun C.S. (ed.), *Proceedings of the Eighth PIMS-MITACS Industrial Problem Solving Workshop PIMS-MITACS IPSW 8*, Pennsylvania State University, 53–66.

Iacopini D., Butler R.W.H., Purves S., McArdle N. & De Freslon N., 2016. Exploring the seismic expression of fault zones in 3D seismic volumes. *Journal of Structural Geology*, 89, 54–73. https://doi.org/10.1016/j.jsg.2016.05.005.

Julien P., Broyer J.L., & Bernet-Rollande O., 2000. Fault Shadow Correction Methodology. [in:] *Proceedings, Indonesian Petroleum Association: Twenty Seventh Annual Convention & Exhibition, October 1999*, Indonesian Petroleum Association, 1–12.

Kallweit R.S. & Wood L.C., 1982. The limits of resolution of zero-phase wavelets. *Geophysics*, 47, 7, 1035–1046. https://doi.org/10.1190/1.1441367.

Karnkowski P., 1993. *Złoża gazu ziemnego i ropy naftowej w Polsce. Tom 1: Niż Polski*. Towarzystwo Geosynoptyków „Geos", Kraków.

Kniesznerr L., Protas A. & Lech S., 1998. Wpływ mezozoicznych naruszeń tektonicznych na własności zbiornikowe dolomitu głównego i migrację węglowodorów w tym poziomie na przykładzie strefy tektonicznej Wysoka Kamieńska – Benice. [w:] *Materiały Konferencji „Najnowsze osiągnięcia w światowej geologii naftowej i ich praktyczne wykorzystanie w Polskim Górnictwie Naftowym i Gazownictwie", Warszawa, 19 Maj 1998*, Biuro Geologiczne GEONAFTA, Warszawa, 77–80.

Kotarba M. & Wagner R., 2007. Generation potential of the Zechstein Main Dolomite (Ca2) carbonates in Gorzów Wielkopolski-Międzychód-Lubiatów area: geological and geochemical approach to microbial-algal source rock. *Przegląd Geologiczny*, 55, 1025–1036.

Kwolek K. & Mikołajewski Z., 2010. Kryteria identyfikacji obiektów litofacjalnych jako potencjalnych pułapek złożowych w utworach dolomitu głównego (Ca2) u podnóża platform i mikroplatform węglanowych w środkowo-zachodniej Polsce. *Przegląd Geologiczny*, 58, 5 426–435.

Li M. & Zhao Y., 2014. *Geophysical Exploration Technology*. Elsevier, Amsterdam.

Li S. & Rao Y., 2020. Poroelastic property analysis of seismic low-frequency shadows associated with gas reservoirs. *Journal of Geophysics and Engineering*, 17, 3, 463–474. https://doi.org/10.1093/jge/gxaa005.

Margrave G.F., 2016. *Attenuation and Deconvolution*. CREWES Research Report, 28, 2016.

Michel L., Flynn M.J. & Hoo C.H., 2011. *Application of PSDM Imaging for Reservoir Characterisation in the Northern Malay Basin: A Case Study*. Paper presented at the International Petroleum Technology Conference, Bangkok, Thailand, November 2011. https://doi.org/10.2523/IPTC-14817-MS.

Mikołajewski Z., 2008. Złoża ropy naftowej w utworach cechsztyńskiego dolomitu głównego (Ca2) w Polsce Północnej. [w:] *Ropa i gaz a skały węglanowe południowej Polski: konferencja naukowo-techniczna: Czarna, 16–18 kwietnia 2008: materiały konferencyjne*, 28.

Mikołajewski Z., Czechowski F. & Grelowski C., 2012. Charakterystyka geologiczno-litologiczno-geochemiczna złóż ropy naftowej w utworach dolomitu głównego w rejonie platformy węglanowej Kamienia Pomorskiego. [w:] *Geopetrol 2012: nowoczesne technologie pozyskiwania węglowodorów w warunkach lądowych i morskich: międzynarodowa konferencja naukowo-techniczna: Zakopane 17–20.09.2012: wydanie konferencyjne*, Prace Naukowe Instytutu Nafty i Gazu, 182, Instytut Nafty i Gazu, Kraków, 387–397.

Mikołajewski Z. & Gamrot J., 2014. Czy złoża w pozaplatformowych utworach dolomitu głównego w NW Polski mają jedynie szczelinową genezę? [w:] *Geopetrol 2014: poszukiwania i eksploatacja złóż ropy naftowej i gazu ziemnego – nowe technologie, nowe wyzwania: międzynarodowa konferencja naukowo-techniczna: Zakopane 15–18.09.2014*, Prace Naukowe Instytutu Nafty i Gazu – Państwowego Instytutu Badawczego, 198, Instytut Nafty i Gazu, Kraków, 405–410.

Nie Y., Jianxin W., Jie Z. & Wei Q., 2012. A forward simulation research to resolve the fault shadow problem. *Energy Procedia*, 16, 97–102. https://doi.org/10.1016/j.egypro.2012.01.018.

Renhai P., Han Q. & Pengye X., 2021. Cases of generalized low-frequency shadows of tight gas reservoirs. *Interpretation*, 9, 1–40. https://doi.org/10.1190/INT-2020-0243.1.

Robertson J.D. & Nogami H.H., 1984. Complex seismic trace analysis of thin beds. *Geophysics*, 49, 4, 344–352. https://doi.org/10.1190/1.1441670.

Słowakiewicz M., Tucker M., Perri E. & Pancost R., 2015. Nearshore euxinia in the photic zone of an ancient sea. *Palaeogeography Palaeoclimatology Palaeoecology*, 426, 242–259. https://doi.org/10.1016/j.palaeo.2016.09.003.

Ślemp P. & Gamrot J., 2013. *Projekt robót geologicznych na obszarze koncesji Kamień Pomorski, Kaleń dla badań sejsmicznych 3D Moracz*. Archiwum PGNiG, Piła [unpublished].

Tai S., Puryear C. & Castagna J., 2009. Local frequency as a direct hydrocarbon indicator. *SEG Technical Program Expanded Abstracts*, 2160–2164. https://doi.org/10.1190/1.3255284.

Taner M.T., 2001. Seismic Attributes. *CSEG Recorder*, 26, 7, 49–56.

Wagner R., 1994. *Stratygrafia osadów i rozwój basenu cechsztyńskiego na Niżu Polskim*. Prace Państwowego Instytutu Geologicznego, 146, PIG, Warszawa.

Wagner R., Dyjaczyński B., Papiernik B., Peryt T.M. & Protas A., 2000. Mapa paleogeograficzna dolomitu głównego (Ca2) w Polsce. [in:] Kotarba M.S. (red.), *Bilans i potencjał węglowodorowy dolomitu głównego basenu permskiego Polski*, Archiwum WGGiOŚ AGH, Kraków.

Wang Y., 2008. *Seismic Inverse Q Filtering*. Blackwell Publishing, London.

Zdanowski P. & Górniak M., 2014. Dim and bright spots as indicators of the Zechstein Main Dolomite hydrocarbon reservoir in Poland. *Interpretation*, 2, 4, 17–30. https://doi.org/10.1190/INT-2014-0039.1.

Zych I. (red.), 2014. *Dokumentacja wyników badań sejsmicznych. Temat: Przetwarzanie i interpretacja danych sejsmicznych Moracz 3D*. Geofizyka Kraków, Kraków [unpublished].